ELSEVIER

Journal of Power Sources 109 (2002) 203–213

JOURNAL OF POWER SOURCES

www.elsevier.com/locate/jpowsour

Modeling viscosity and conductivity of lithium salts in γ-butyrolactone

A. Chagnes[a,*], B. Carré[a], P. Willmann[b], D. Lemordant[a]

[a]*Laboratoire de Physicochimie des Interfaces et Milieux Réactionnels (EA2048), Université de Tours, Faculté des Sciences et Techniques, Parc de Grandmont, F 37200 Tours, France*

[b]*CNES, 18 Avenue E. Belin, F 31055 Toulouse Cedex, France*

Received 20 October 2001; received in revised form 12 January 2002; accepted 22 January 2002

Abstract

Viscosity and conductivity properties of Li-salts (lithium tetrafluoroborate ($LiBF_4$), lithium hexafluorophosphate ($LiPF_6$), lithium hexafluoroarsenate ($LiAsF_6$), lithium bis-(trifluoromethylsulfone)-imide (LiTFSI)) dissolved in γ-butyrolactone (BL) have been investigated. The *B*- and *D*-coefficients of the Jones–Dole (JD) equation for the relative viscosity of concentrated electrolyte solutions (concentration: $C = 0.1$–1.5 M): $\eta_r = 1 + AC^{1/2} + BC + DC^2$, have been determined as a function of the temperature. The *B*-coefficient is linked to the hydrodynamic volume of the solute and remains constant within the temperature range investigated (25–55 °C). The *D*-coefficient, which originates mainly from long-range coulombic ion–ion interactions, is a reciprocal function of the temperature. The variations of the molar conductivity (Λ) with *C* follow the cube root law $\Lambda = \Lambda^{0'} - S'C^{1/3}$ issued from quasi-lattice theory of electrolyte solutions. From the Walden product $W = \Lambda\eta$ which does not vary with *C* and the JD equation, the bell shape of the conductivity–concentration relationship is explained and it is shown that the concentration in salt at the maximum of conductivity is linked to the *D*-coefficient. Raman spectroscopy has been used as an additional tool to investigate ion pairing in BL. Ions pairs have been evidenced for $LiClO_4$ solutions in BL but not for $LiPF_6$. As little variations occur for the ions pairs dissociation coefficient when the salt concentration is increased, the cube root law remains valid, at least in the concentration range investigated.

Keywords: Quasi-lattice theory; Viscosity; Conductivity; Organic electrolytes; Butyrolactone; Lithium battery

1. Introduction

Viscosity and conductivity of electrolyte solutions are related to transport processes and play an important role in the field of lithium batteries as the knowledge of the conductivity is necessary for the design of Li cells. Viscosity and conductivity measurements, provide also useful insights on ion solvation and association. At the present time, the mechanisms of ion transport in concentrated organic electrolytes is not clearly understood. The lack of convenient theories is evident and only empirical relations have been proposed. As an example, the extended Jones–Dole (JD) equation [1] for the relative viscosity of solutions (η_r) has been extensively used to describe the viscosity variations of electrolyte solutions when the concentration of the salt (*C*) is varied:

$$\eta_r = \eta/\eta_0 = 1 + AC^{1/2} + BC + DC^2 \quad (1)$$

In this equation, η and η_0, are the viscosities of the solution and the pure solvent respectively, and *A*, *B* and *D* are the coefficients. This first term, in $C^{1/2}$, on the right hand side of Eq. (1), is linked to the interaction of a reference ion with its ionic atmosphere and may be calculated by the Falkenhagen theory [2] but, usually, this term vanished in organic solvents when the concentration in salt is raised above $C \approx 0.05$ M. The *BC* term is predominant at $C > 0.05$ M and has been attributed to ion–solvent interactions as well as to volume effects [3]. The third term in C^2, appears at the highest concentrations in salt (0.5–2 M or more), i.e. when the mean interionic distance decreases and becomes of the order of magnitude of a few solvent molecules diameters. It is mainly related to ion–ion and/or ion–solvent interactions as it does not appear in the case of weak electrolytes [4].

Variations of the molar conductivity (Λ) of diluted electrolytes solutions with salt concentration are usually described by the classical Debye–Hückel–Onsager (DHO) equation: [5,6]

$$\Lambda = \Lambda^0 - SC^{1/2} \quad (2)$$

where Λ^0 is the molar conductivity at infinite dilution and *S*, a calculable parameter which depends on both the physical

* Corresponding author. Fax: +33-2-47-36-69-60.
E-mail addresses: chagnes@univ-tours.fr (A. Chagnes), lemordant@univ-tours.fr (D. Lemordant).

0378-7753/02/$ – see front matter
PII: S0378-7753(02)00073-3

properties of the solvent and the nature of the electrolyte. Nevertheless, experimental results indicate that the Eq. (2) is not followed [7,8], excepted at very low concentration ($C < 0.001$ M) and, even in these conditions, the experimental slope (S_{exp}) is often different (higher or lower) than the calculated one (S_{calc}) [8]. Attempts to correct experimental result for solution viscosity and ion association are not successful and the discrepancies between theory and experience remain [9]. Clearly, in concentrated organic electrolytes, the conductivity process is different from the model embodied in the DHO equation. Another approach has been provided by the use of the quasi-lattice theory [10,11]. This theory, adapted for conductivity [12], has been applied successfully to the system γ-butyrolactone (BL) + $LiClO_4$ [7]. According to this theory, the variations of Λ with C are described by the following equations:

$$\Lambda = \Lambda^{0\prime} - S'C^{1/3} \tag{3}$$

where

$$S' = S_1 + S_2\Lambda^{0\prime} \tag{4}$$

$$S_1 = \frac{0.293e^2M(2N_a)^{1/3}}{4\pi\varepsilon_0\varepsilon_r k_b T} \tag{5}$$

and

$$S_2 = \frac{e^2MN_a(2N_a)^{1/3}}{\pi\eta} \tag{6}$$

In these equations, ε_0 is the permittivity of free space, ε_r the relative permittivity of the solvent, e the electronic charge, T the temperature, k_b the Boltzmann's constant, N_a the Avogadro's number, and M the lattice parameter (equivalent to a Madelung constant). $\Lambda^{0\prime}$ (S cm^{-1}) is the molar conductivity of the salt at infinite dilution given by the lattice model. As this model is from different ground from the Debye and Hückel ones, the values $\Lambda^{0\prime}$ and Λ^0, obtained by extrapolation, respectively, from the $C^{1/3}$ and $C^{1/2}$ law, may differ. As the relaxation term S_1 is usually greater than the electrophoretic term S_2, the slope of the $\Lambda = f(C^{1/3})$ relation is mainly dependent on the lattice parameter value M and the temperature.

Propylene carbonate (PC) and BL are popular dipolar aprotic solvents widely used for storage energy or electrochromic devices. For practical applications, the lower viscosity of BL over PC overrides its lower permittivity. The two oxygen atoms of BL act as bidentate ligand toward small cations like Li^+ [13] and prevent the formation of non-conducting contact ion-pairs. As a result, the moderate viscosity of BL and the limited ion aggregation are responsible for the high conductivity in liquid electrolytes as well as in PMMA-based gels [14]. Li-salts having large anions lead to a reduction of ionic association and thus, to an increase in conductivity and solubility: lithium tetrafluoroborate ($LiBF_4$), lithium hexafluorophosphate ($LiPF_6$), lithium hexafluoroarsenate ($LiAsF_6$), lithium bis-(trifluoromethylsulfone)-imide (LiTFSI) are mainly used in practice.

The purpose of the present paper is to examine whether the preceeding Eqs. (1), (3)-(6) may be applied to other salts than $LiClO_4$. For this purpose, viscosity and conductivity measurements of $LiBF_4$, $LiAsF_6$, $LiPF_6$ and LiTFSI solutions in BL have been performed. All these lithium salts are widely used in the field of lithium batteries as organic electrolytes. Viscosity measurements have been realised from 25 to 55 °C and in a sufficiently wide range of concentration to determine accurately the B- and D-coefficients of the JD equation as a function of the temperature. The validity of the cube root law for the variation of the conductivity with concentration (Eq. (3)) has been tested for these electrolyte solutions. From the temperature dependence of the viscosity and the conductivity, the corresponding activation parameters $E_{a,\eta}$ and $E_{a,\Lambda}$ have been determined as a function of the salt concentration. Raman spectroscopy is a useful tool to study short range ion–ion interactions, leading to the possible formation of ion-pairs and higher ionic aggregates. Raman spectroscopy is presently used to investigate ion association in BL.

2. Experimental

BL (purity > 99%) was obtained from Aldrich and dried over molecular sieves prior to use. $LiClO_4$ (99%), $LiPF_6$ (98%), $LiAsF_6$ (98%), $LiBF_4$ (99%), LiTFSI (99%) were obtained from Fluka and dried in a vaccum oven before dissolution in the solvents. The water content of the solutions was <50 ppm as indicated by Karl Fisher titration.

AC conductivity measurements were carried out using a conductivity cell with platinum electrodes and a Philips

Table 1
Variations of the density (g cm^{-3}) of $LiBF_4$, $LiPF_6$, $LiAsF_6$, and LiTFSI solutions in BL with temperature and salt concentration

$LiBF_4$ (°C)	0.1 M	0.2 M	0.5 M	0.75 M	1 M	1.5 M
25	1.130	1.134	1.149	1.161	1.173	1.196
35	1.120	1.125	1.140	1.152	1.164	1.188
45	1.112	1.118	1.133	1.144	1.157	1.181
55	1.105	1.109	1.125	1.136	1.150	1.174
$LiPF_6$ (°C)	0.2 M	0.5 M	0.75 M	1M	1.5 M	
25	1.135	1.163	1.186	1.207	1.261	
35	1.128	1.154	1.178	1.198	1.252	
45	1.121	1.146	1.170	1.191	1.244	
55	1.113	1.139	1.162	1.185	1.237	
$LiAsF_6$ (°C)	0.125 M	0.25 M	0.5 M	1.5 M		
25	1.169	1.157	1.185	1.316		
35	1.131	1.148	1.177	1.308		
45	1.122	1.140	1.169	1.299		
55	1.114	1.133	1.162	1.289		
LiTFSI (°C)	0.1 M	0.2 M	0.5 M	0.75 M	1 M	1.5 M
25	1.139	1.147	1.183	1.220	1.253	1.318
35	1.128	1.137	1.173	1.203	1.243	1.303
45	1.120	1.129	1.157	1.201	1.235	1.297
55	1.113	1.122	1.147	1.194	1.228	1.285

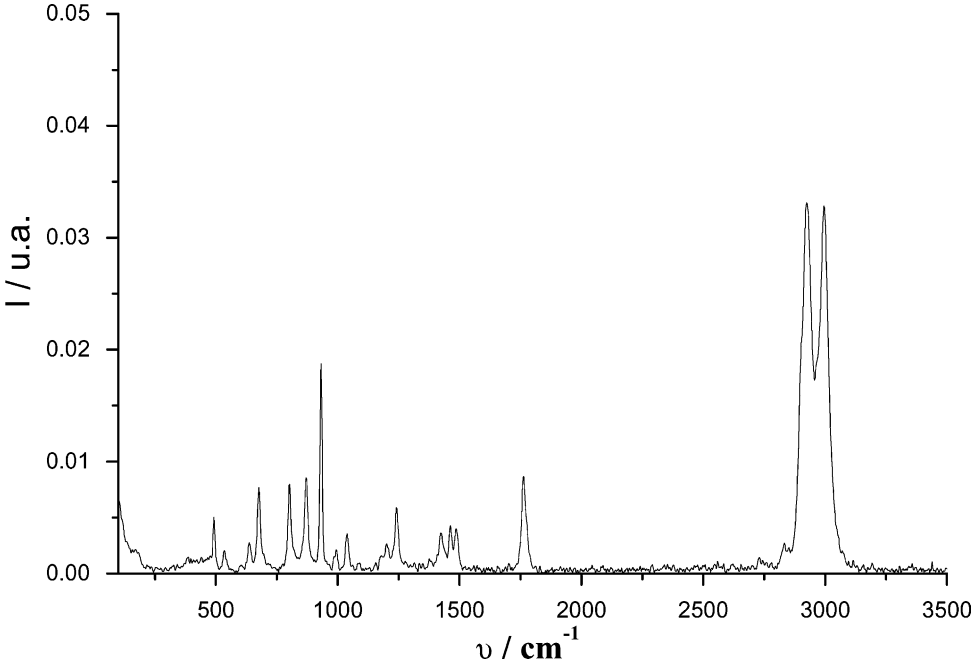

Fig. 1. Raman spectrum of pure BL.

PM6303 impedance analyser operating at 1000 Hz. Viscosity measurements were obtained using an Ubbelhode capillary tube immersed in a thermostated bath (±002 °C) and a Schott viscometer(AUS 310). The densities of solutions, required to calculate the dynamic viscosities, were determined using a vibrating tube densimeter (Picker) and results are reported in Table 1.

The Raman spectra were recorded with a Bruker RFS100 spectrometer. The near-infrared laser was operating at a wavelength of 1064 nm with a power on the sample of 100 mW and a light spot of 0.1 mm in diameter. The scattered light was collected at 180° from the direction of the incident light. Each Raman spectrum was the result of 100 scans. The germanium detector was cooled in liquid nitrogen and an OS/2 operating system was used to collect and process data. Optical glass test tubes were used for Raman measurements. In Fig. 1, is reported the Raman spectra of pure BL. All the spectra have been normalised using the C–H elongation of BL at 3000 cm^{-1} because this band present a high intensity and does not interfere with others studied bands. In the following, the contribution of BL to Raman spectra has been removed by subtraction.

3. Results and discussion

3.1. Viscosity

The variations of the viscosity at 298 K of $LiBF_4$, $LiPF_6$, $LiAsF_6$, and LiTFSI solutions in BL are plotted against the salt concentration in Fig. 2. The variations in viscosity of the solutions are very similar, excepted for $LiBF_4$ which is the salt with the smallest anion and the most susceptible to be affected by ion pairing.

In order to determine precisely the *B*- and *D*-coefficients in the JD equation, the following procedure has been employed. A plot of $(\eta_r - 1)/C$ against C forces all higher interaction terms to be absorbed in the slope [15,16] and the ordinate at $C = 0$ gives a precise value of B. The D-coefficient was subsequently determined by a least square method. *B*- and *D*-values obtained by this method, in the temperature range 25–55 °C, are given in Table 2.

The *B*-coefficients vary with the nature of the anion but not with the temperature, at least in the temperature range investigated, and for each salt, a mean value has been calculated. As indicated by the S.D. of the mean, the observed variations are in the order of the experimental error. At the opposite, the *D*-coefficients decrease regularly with temperature and in order to investigate the exact nature of the temperature dependency of D, we have plotted D values against $1/T$. All the $D = f(1/T)$ curves reported in Fig. 3 are linear. The slopes P of D versus $1/T$ for each salt are also gathered in Table 2. The fact that D is more sensitive to thermal agitation than B is not surprising since B is mainly related to the hydrodynamic volume (including solvation effects, refer to the following paragraph) and D mostly to ion-dipoles interactions and long range coulombic ion–ion interactions.

The BC term in the JD equation may be also deduced from the hydrodynamic equation proposed by Einstein for the relative viscosity of spherical unsolvated particles [17]:

$$\eta_r = 1 + 2.5\Phi + o(\Phi^2) \quad (7)$$

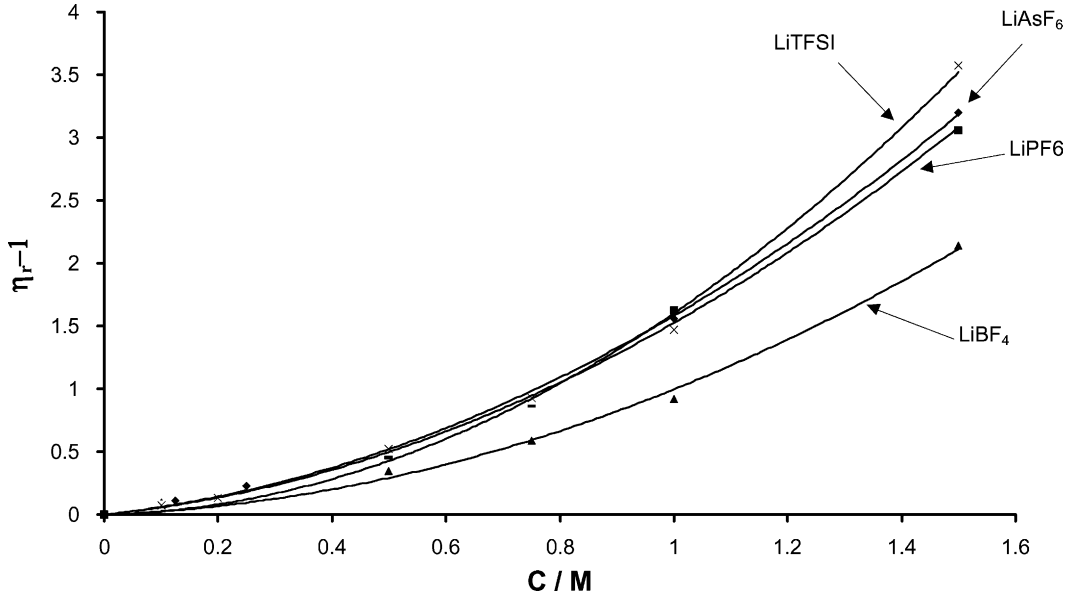

Fig. 2. Variations of the viscosity of $LiBF_4$, $LiPF_6$, $LiAsF_6$ and LiTFSI solutions in BL with salt concentration at 25 °C.

In Eq. (7), Φ is the volume fraction of the particles in the fluid. As Φ can be expressed as a function of the concentration C and the hydrodynamic molar volume V_i of the particles, Eq. (7) may be rewritten as:

$$\eta_r = 1 + 0.0025 V_i C + o(C^2) \quad (8)$$

when V_i is in $cm^3\ mol^{-1}$ and terms in C^2 and higher are considered as negligible. If it is supposed that this equation holds at the molecular scale for large solute molecules, identification of Eqs. (1) and (8) leads to $B_{calc} = 0.0025\ V_i$. Using this relation, ones can deduce B_{calc} from the solvated volume of the electrolyte V_i. B_{calc} values, reported in Table 2, are obtained by taking $r(Li^+)_{solv} = 0.346$ nm for the solvated radius of the Li ion [7,18] and $r(anion) = 0.227$ nm (BF_4^-), 0.254 nm (PF_6^-), 0.259 nm (AsF_6^-), and 0.326 nm ($TFSI^-$) in literature [18]. The agreement between experimental and calculated values of B is good which means that the volume effect is predominant, at least for large anions and strongly solvated cations.

3.2. Activation energy for the viscous flow

From Eyring's theory of activated processes [19], an expression for the variations of solutions viscosity with temperature is:

$$\eta = \frac{hN_a}{V_m} \exp\left(\frac{\Delta S^{\neq}}{R}\right) \exp\left[\frac{\Delta H^{\neq}}{RT}\right] \quad (9)$$

In Eq. (9), h is the Planck's constant, V_m the molar volume of solvent (76.6 $cm^3\ mol^{-1}$ for BL), $\Delta S^{\neq}$ the activation entropy and $\Delta H^{\neq}$ the activation enthalpy, generally identified to the activation energy of the viscous flow $E_{a,\eta}$. Non-associated solvents and non glass-forming ionic and molecular liquids, usually verify this equation.

We have reported in Table 3 the values of the activation energy and entropy for the viscous flow of $LiBF_4$, $LiPF_6$, $LiAsF_6$, and LiTFSI solutions in BL. In a preceding work [7], a linear relation between the activation energy for the viscous

Table 2
B (M^{-1}) and D (M^{-2}) coefficients of the JD equation and slope ($P/M^{-2}K$) of the $D = f(1/T)$ relation for $LiBF_4$, $LiPF_6$, $LiAsF_6$ and LiTFSI solutions in BL

T (°C)	$LiBF_4$		$LiPF_6$		$LiAsF_6$		LiTFSI	
	B	D	B	D	B	D	B	D
25	0.30	0.75	0.40	1.10	0.40	1.15	0. 50	1.20
35	0.30	0.70	0.40	0.95	0.42	1.00	0.47	1.10
45	0.30	0.65	0.38	0.85	0.42	0.85	0.46	1.05
55	0.25	0.55	0.42	0.68	0.41	0.75	0.50	0.90
B_{mean}	0.288 ±0.013	–	0.400 ±0.008	–	0.413 ±0.005	–	0.483 ±0.013	–
B_{calc}[a]	0.33	–	0.36	–	0.37	–	0.48	–
P		630		1330		1320		930

[a] $B_{calc} = 0.0025\ V_i$ (at 25 °C, refer to text).

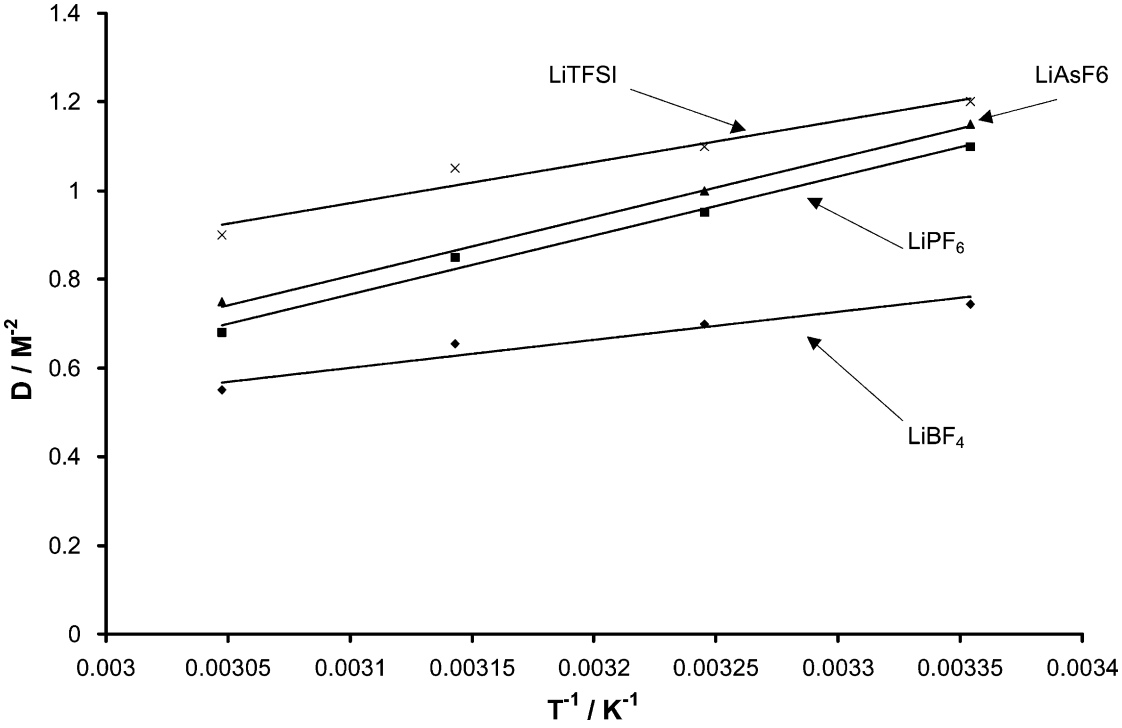

Fig. 3. Variation of the D-coefficient in the JD relation (Eq. (1) in the text) with $1/T$.

flow $E_{a,\eta}$ and the salt concentration C has been proposed:

$$E_{a,\eta} = E^0_{a,\eta} + V_m E^{salt}_{a,\eta} C \quad (10)$$

where $E^0_{a,\eta}$ and $E^{salt}_{a,\eta}$ respectively, are the energy of activation for the pure solvent and the contribution of the salt (per mole of the solute) to the activation energy for the transport process.

Table 3
Activation energy $E_{a,\eta}$ (kJ mol^{-1}) and entropy $\Delta S^{\neq}$ (J K^{-1} mol^{-1}) for the viscous flow of $LiClO_4$, $LiBF_4$, $LiPF_6$, LiTFSI and $LiAsF_6$ solutions in BL

	C/M					
	0	0.1	0.2	0.5	1.0	1.5
$LiClO_4$[a]						
$E_{a,\eta}$	10.7	11.1	11.5	12.6	14.8	16.3
$\Delta S^{\neq}$	−12.2	−11.4	−10.8	−9.3	−5.5	−4.7
$LiBF_4$						
$E_{a,\eta}$	10.7	13.1	13.3	14.4	15.5	17.2
$\Delta S^{\neq}$	−12.2	−4.4	−2.8	−2.3	−1.3	−0.4
$LiPF_6$						
$E_{a,\eta}$	10.7	11.1	12.0	14.0	17.7	19.5
$\Delta S^{\neq}$	−12.2	–	−8.9	−4.4	1.9	5.3
LiTFSI						
$E_{a,\eta}$	10.7	11.3	11.7	12.5	14.5	17.5
$\Delta S^{\neq}$	−12.2	−9.4	−4.5	−2.5	0.2	5.6
$LiAsF_6$						
$E_{a,\eta}$	10.7	12.0	12.4	12.7	15.6	17.3
$\Delta S^{\neq}$	−12.2	−8.8[b]	−8.1[c]	−9.0	−3.6	−2.0

[a] [7].
[b] $C = 0.125$ M.
[c] $C = 0.25$ M.

In Fig. 4, we have reported the variations of $E_{a,\eta}$ with C for the different salts under study. Only for $LiBF_4$, the ordinate at the origin is different from $E^0_{a,\eta} = 10.7$ kJ mol^{-1}. From the slopes of the lines, $E^{salt}_{a,\eta}$ values, in kJ mol^{-1}, have been infered: 38 ($LiBF_4$), 81 ($LiPF_6$), 60 ($LiAsF_6$) and 56 (LiTFSI). Since $E^{salt}_{a,\eta}$ ($LiClO_4$) = 49.3 kJ mol^{-1} [7], it appears that the nature of the anion has a strong influence on $E^{salt}_{a,\eta}$, BF_4^- and PF_6^- leading respectively, to the lowest and the largest values. One may notice, that the most the salt is expected to be associated in ion-pairs (especially in the case of small anions bearing localized charge), the most the slope and hence $E^{salt}_{a,\eta}$ is low. Ions pairs will probably contribute less to the increase in viscosity of electrolyte solutions than free ions.

The activation entropy $\Delta S^{\neq}$ for the viscous flow can be deduced from experimental viscosities using Eq. (9). As shown in Table 3, all values increase when the salt is added and at $C = 1.5$ M follow the order:

$$\Delta S^{\neq}(LiPF_6) \approx \Delta S^{\neq}(LiTFSI) > \Delta S^{\neq}(LiBF_4) > \Delta S^{\neq}(LiAsF_6) > \Delta S^{\neq}(LiClO_4)$$

In all instances, an increase of $\Delta S^{\neq}$ is observed when the salt is added to the pure solvent. This means that the presence of the salt induced a decrease in order in the transition state relatively to the initial state. As it is considered that the presence of the salt at high concentration induces the formation of a ionic quasi-lattice (vide infra), a decrease in entropy and consequently a sharp increase in order in the initial state is expected. This could contribute to explain the observed increase in activation entropy

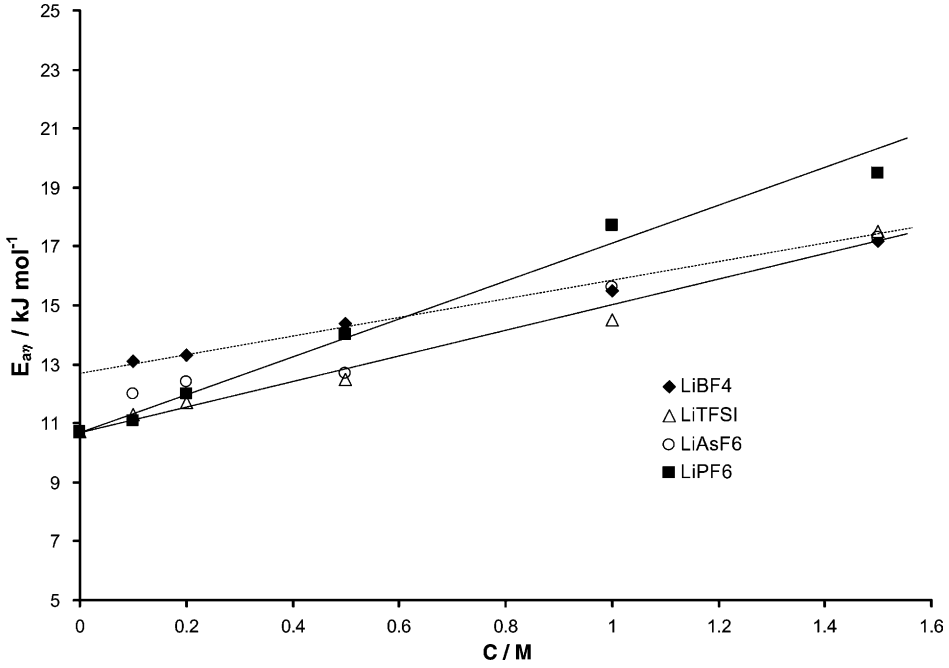

Fig. 4. Activation energy for the viscous flow ($E_{a\eta}$) vs. salt concentration (C) for $LiBF_4$, $LiPF_6$, $LiAsF_6$ and LiTFSI solutions in BL.

(Fig. 5). Nevertheless, it cannot be excluded that the entropy of the transition state itself is affected by variations in ionic strength.

3.3. Conductivity

3.3.1. Variation of the molar conductivity with concentration

The molar conductivities (Λ), are deduced from the experimental conductivities (K) by $\Lambda = K/C$. In Fig. 6, the variations of Λ for $LiBF_4$, $LiPF_6$, $LiAsF_6$ and LiTFSI have been plotted against the cube root of the salt concentration in BL. As expected from Eq. (3), linear plots are obtained for all salts under consideration.

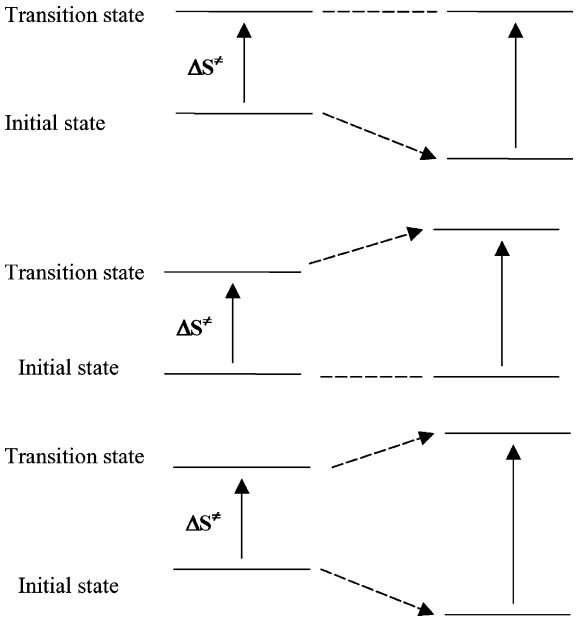

Fig. 5. Possible variations of the entropy of activation for the viscous flow ($\Delta S^{\neq}$) in the presence of a dissolved salt.

According to the quasi-lattice theory, first introduced by GOSH [10] and developed further by Bahe [20], the Debye length κ_D in the ionic cloud model may be replaced, when the ionic strength is raised above 0.1 M (as for these electrolytes), by κ_L the average distance between ions of opposite charge, supposed to be distributed on the vertices of an expanded lattice [21]:

$$\kappa_L = M(2000 N_a C)^{1/3} \tag{11}$$

In Eq. (11), the salt concentration C is expressed in mol l^{-1}. In a similar manner, the usual DHO conductivity equation may be adapted by introducing the parameter κ_L instead of κ_D as proposed by Smith [22]. Then, the variations of the molar conductivity with concentration are described by Eq. (3). If all parameters in Eqs. (3)–(6) are known, S′ for a given salt–solvent system can be calculated (S'_{calc}) and compared to the experimental value (S'_{exp}). S'_{calc}, S'_{exp}, $\Lambda^{\circ\prime}$ and Λ° values are gathered in Table 4. S'_{calc} has been calculated using the Madelung constant for the fcc lattice: $M = 1.74$. For comparison, values obtained for $LiClO_4$ in BL [7] and propylene carbonate (PC) have been added [23]. It is noticeable that S'_{calc} values are close to S'_{exp} for all salts under study, as previously found for $LiClO_4$ in BL [7]. Nevertheless, as there is no particular reason for the ions to adopt a regular fcc lattice, the constant M may be best regarded as an adjustable parameter. Using experimental data, M values have been adjusted to experimental data and reported in Table 4. All values fall in the range 1.5–2.4, with

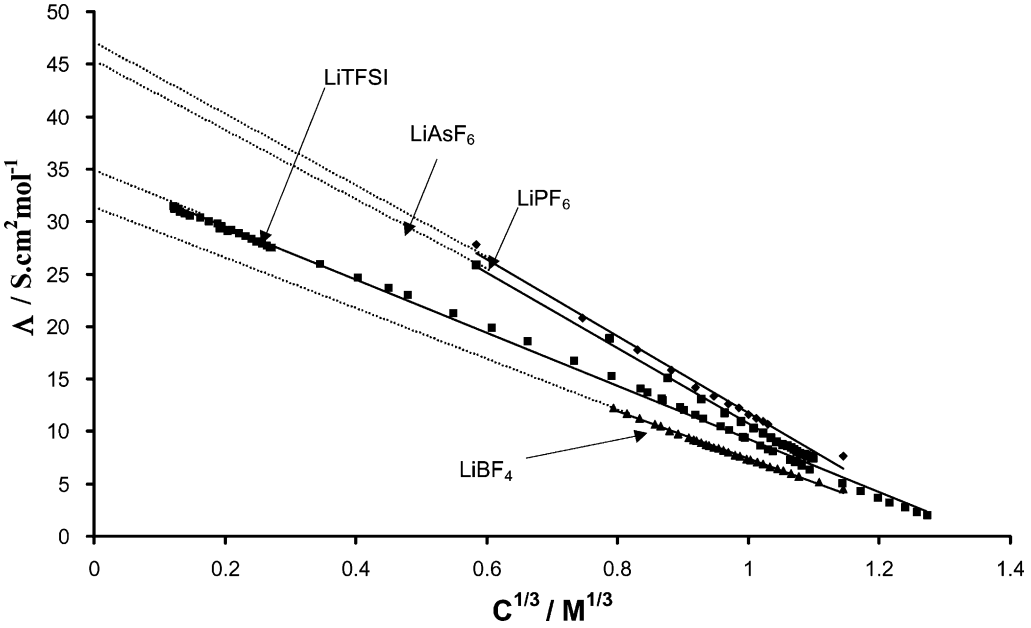

Fig. 6. Plot of the molar conductivity Λ vs. the cube root of the concentration $C^{1/3}$ (C expressed in mol l^{-1}) for $LiBF_4$, $LiPF_6$, $LiAsF_6$ and LiTFSI solutions in BL.

a mean of 2.0, not to different from 1.74, the rock–salt value. $\Lambda^{\circ\prime}$ and Λ° values do not differ significantly, excepted for $LiBF_4$. As it has been reported that the dissociation coefficient of $LiBF_4$ (1 M) at 25 °C in BL is 0.34 [24], BL solutions of this salt may involve contact ion-pairs, leading to a possibly underestimated value for the ordinate in the $\Lambda = f(C^{1/3})$ plot.

3.4. Maximum of conductivity

When the concentration in salt is raised, the number of charge carriers increases but, at the same time, the viscosity increases as indicated by the JD relation. The consequence is that the ionic mobilities inevitably decrease. The competition between the increase in number of charge carriers and the decrease of their mobilities lead to a maximum in the conductivity–concentration relationship. This maximum is usually obtained around 1 M in organic electrolytes. For evident reasons, the determination of this maximum in conductivity is important for batteries applications.

The maximum conductivity value (C_{max}) is easily deduced from Eq. (3) by derivation of K relatively to the concentration:

$$C_{max} = \left(\frac{3\Lambda^{0\prime}}{4S'}\right)^3 \quad (12)$$

C_{max} is then related to the molar conductivity at infinite dilution $\Lambda^{0\prime}$ and to the slope of the $\Lambda = f(C^{1/3})$ plot which can be calculated as previously indicated (Eqs. (4)–(6)).

An alternative way to determine C_{max} is provided by the study of the variations of the Walden product $W = \Lambda\eta$ with salt concentration. In the present electrolyte solutions, W is approximately constant as indicated by the Ln $\eta = f(\text{Ln}\ \Lambda)$ plot reported in Fig. 7. Straight lines are obtained whose slope ranges from −0.8 to −1 when the concentration is varied from 0.2 to 1.5 M. Introducing the JD equation and W in the expression of the conductivity of electrolyte solutions leads to:

$$K = \Lambda C = \frac{WC}{\eta} = \frac{WC}{(\eta^0(1 + BC + DC^2))} \quad (13)$$

Eq. (13) has a maximum for:

$$C_{max} = \frac{1}{D^{1/2}} \quad (14)$$

In Table 5 are reported, the concentration at maximum of conductivity obtained from experimental data and values calculated by Eqs. (12) and (14). As expected, a good

Table 4
Slopes (S') and ordinates ($\Lambda^{\circ\prime}$) in the correlation $\Lambda = f(C^{1/3})$ (Eq. (3) in the text) for $LiBF_4$, $LiPF_6$, $LiAsF_6$ and LiTFSI in BL and LiTFSI in PC at 25 °C

	BL				PC
	$LiBF_4$	$LiPF_6$	$LiAsF_6$	LiTFSI	LiTFSI
S'	22.92	36.55	36.00	26.47	19.32
S'_{calc}	23.54	37.55	36.34	27.77	11.65
$\Lambda^{0\prime}$	30.29	48.32	46.77	35.74	24.69
Λ^0	42.64[a]	40.73[a]	39.91[a]	33.77[a]	23.80[a]
$\Lambda^{0\prime}/\Lambda^0$	0.71	1.18	1.17	1.06	1.04
M	1.48	2.40	2.12	1.86	2.28

Λ° is the limiting molar conductivity given by the DHO relation. Eqs. (4)–(6) have been used to obtain S'_{calc}. M represents the value of the optimized lattice parameter.

[a] [18].

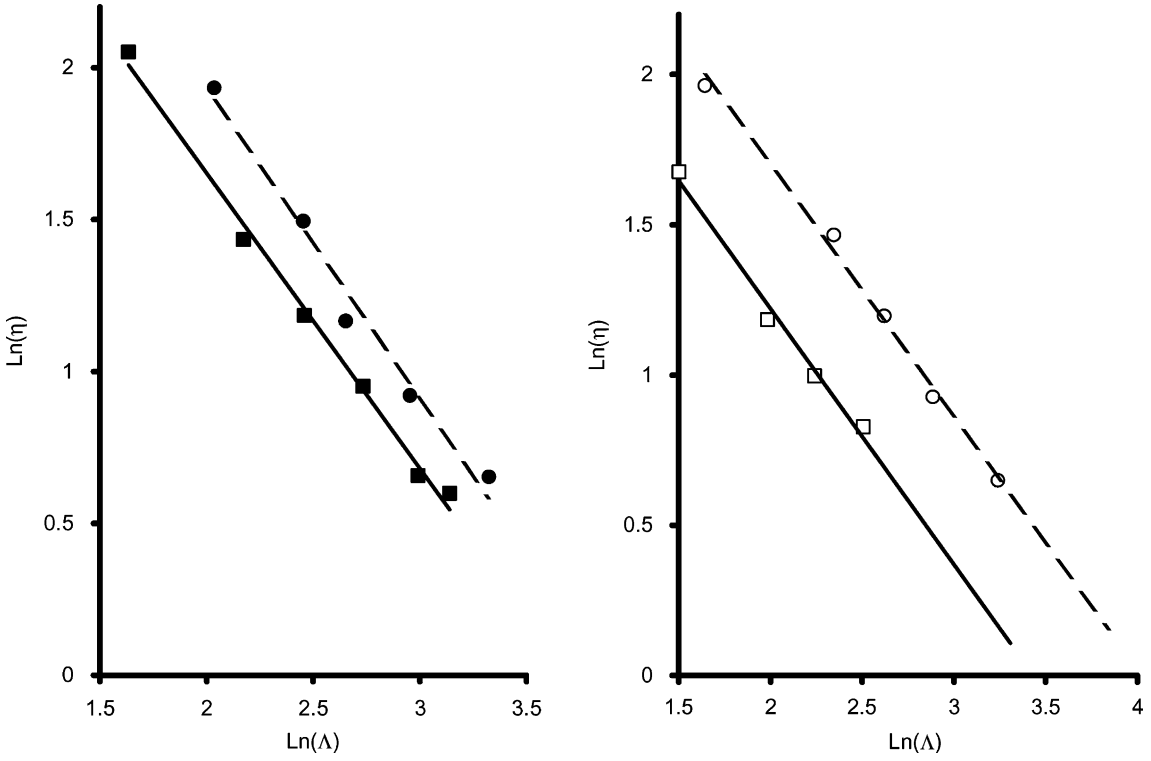

Fig. 7. Ln $\Lambda = f(\text{Ln } \eta)$ for $LiBF_4$, $LiPF_6$, $LiAsF_6$ and LiTFSI solutions at 25 °C in BL.

agreement is obtained between calculated and experimental values, and it can be noted that C_{max} value can be predicted using only $\Lambda^{0\prime}$ as experimental entry (approximated by Λ^0 if necessary) as all others parameter involved in S' may be calculated (for M the fcc value is used) or alternatively deduced from viscosity measurements.

As the quasi-lattice model disregards the formation of non-conducting contact ion-pairs, this theory cannot be readily extended to all organic electrolytes, especially those having low permittivity. This problem will be considered in a following paragraph.

3.5. Activation energy for conductivity

According to the Eyring's theory, viscosity and conductivity are both activated transport processes. From the quasi-lattice theory, a relation between the activation energy for the conductivity ($E_{a,\Lambda}$) and the salt concentration may be inferred [7]:

$$E_{a,\Lambda} = E^0_{a,\Lambda} + kC^{4/3} \tag{15}$$

where k is given by:

$$k = \frac{2N_a^{4/3}e^2V_mM10^4}{(4\pi\varepsilon_0\varepsilon_r Z^{1/3})} \tag{16}$$

In this expression, Z is the number of ions in a unit cell of the cation (or anion) sub-lattice. $E_{a,\Lambda}$ versus $C^{4/3}$ has been plotted on the graphs reported in Fig. 8. As previously found for the BL–$LiClO_4$ system [7], the variations of $E_{a,\Lambda}$ for $LiBF_4$, $LiAsF_6$, $LiPF_6$ and LiTFSI follow Eq. (15). Experimental slopes (k) and ordinate ($E^0_{a,\Lambda}$) values obtained by linear regression for the different salts are reported in Table 6. The ordinate of the correlation $E^0_{a,\Lambda}$, which represents the infinitesimal dilution activation energy for the conductivity, reaches a value which is close to the activation energy for the viscosity of pure BL (10.7 kJ mol^{-1}). At infinitesimal dilution, the activation energy for the conductivity represents the interactions of one mole of ''discharged'' ions (their distance is considered as to large for even long range interaction to occur). Taking $M = 1.74$ and $Z = 4$, k_{calc} given by Eq. (14) is 0.5 kJ $(mol/l)^{-4/3}$. There is no agreement between experimental and calculated k values. The smallest k value is obtained for $LiBF_4$. This lack of agreement indicates that others interactions than coulombic forces between ions of opposite charge have to be taken into

Table 5
Salt concentration at the maximum of conductivity (C_{max} in M) at 25 °C in BL. Eqs. (12) and (14) are used for calculated values

Salts	C_{max}	C_{max} [a]	C_{max} [b]	κ (mS/cm)
$LiBF_4$	1.02	0.90	1.15	7.33
$LiPF_6$	0.98	0.90	0.95	11.63
$LiAsF_6$	1.01	0.90	0.93	10.48
LiTFSI	0.97	0.90	0.91	9.21

[a] Given by Eq. (12).
[b] Given by Eq. (14).

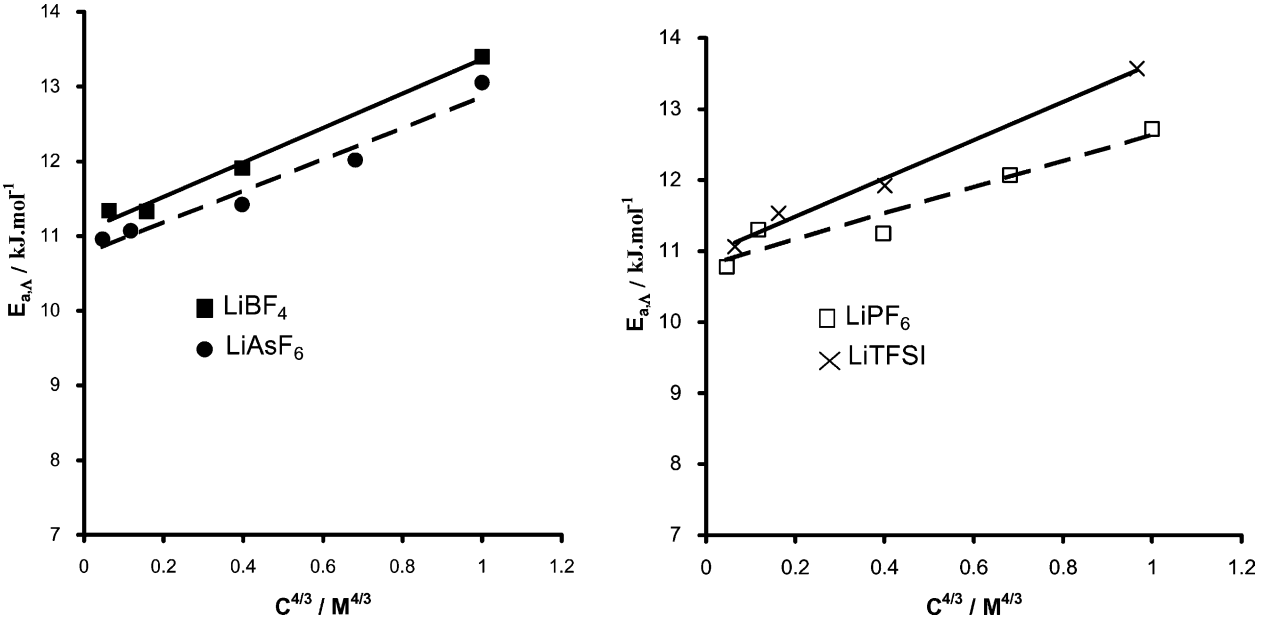

Fig. 8. Activation energy for conductivity $E_{a\Lambda}$ vs. $C^{4/3}$ for $LiBF_4$, $LiPF_6$, $LiAsF_6$ and LiTFSI in BL.

account to obtain a quantitative agreement between theory and experience. As a matter of fact, the ion–solvent dipole interactions energies must be quite high in media containing strongly dipolar solvents like cyclic carbonates or lactones.

3.6. Ion association

In 1926, Bjerrum [25] introduced the notion of ion-pairs formed by the following chemical equilibrium:

$$A^+ + B^- \rightarrow (A^+, B^-)$$

This equilibrium is characterized by the thermodynamical association constant K_a:

$$K_a = \frac{(1-\alpha)}{(\alpha^2 C \gamma_\pm{}^2)} \quad (17)$$

In Eq. (17), $\gamma_\pm$ is the mean activity coefficient and α the ion pair dissociation coefficient. In diluted solutions, K_a is determined using the DHO treatment for α and the Debye and Hückel law for $\gamma_\pm$. At high ionic strength ($I > 0.05$ M), the use of the preceding equations is not possible and the determination of both α and $\gamma_\pm$ is problematic. For these reasons, the ion and ion-pair concentrations, but not the activities, are best determined spectrocopically using IR or Raman spectroscopy. Associated species like contact ion-pairs ($Li^+ \ldots X^-$) are easily detected by Raman spectroscopy [26], but the existence of solvent separated ions pairs ($Li^+ \ldots S \ldots X^-$) remains questionable. The formation of associated species depends strongly of the nature of the solvent used. As an example, $LiAsF_6$ remains fully dissociated in PC [26] but in dimethyl carbonate (DMC) the following species have been detected [26]: free Li^+ and AsF_6^- ions, contact ion-pairs [$Li^+ \ldots AsF_6^-$], solvated ion-pairs [$Li(DMC)_4]^+ \ldots AsF_6^-$ and polymeric ion-pairs [$Li^+ \ldots AsF_6^-]_x$. Even in high permittivity solvents, contact ion-pairs may be formed when the salt concentration is increased. This is in particular the case of $LiClO_4$ in PC [27].

Table 6
Slopes of the $E_{a\Lambda} = f(C^{4/3})$ (kJ mol^{-1}) relationship and activation energy at infinite dilution (Eq. (15) in the text)

	Salts			
	$LiBF_4$	$LiPF_6$	$LiAsF_6$	LiTFSI
$k_{exp}/M^{-4/3}$	1870	2120	2300	2690
$E^0_{a,\Lambda}$	10.8	10.7	11.0	10.9

Ion association in BL has been investigated for $LiPF_6$, and $LiClO_4$ as no association is expected for the $TFSI^-$ anion which has the largest delocalized structure. In fact, it has been observed by Raman spectroscopy for LiTFSI in BL [28] that unperturbated BL molecules at 676 cm^{-1} coexist with molecules in strong interaction with Li^+ ion at 690 cm^{-1}. The solvation number of Li^+ ions found by Raman is 4 and from this study, it results that only free ions and possibility solvent separated ions pairs may exist in LiTFSI/BL solutions. In Fig. 9 is reported the Raman spectra of solid $LiPF_6$ (as powder) and $LiPF_6$ in BL at 0.5 and 1.5 M. The peaks have a Gaussian shape and the area (A) under the curves is a linear function of the salt concentration: $A = 0.0285C$, with a regression coefficient $r = 0.91$. There is no evidence of a new emission band which could be attributed to ion-pairing. As a conclusion, if ions pairs are formed at high concentration in salts, these would be solvent separated or solvent–solvent separated ion-pairs.

Fig. 10 shows the Raman spectra of BL in the presence of 1 and 1.5 M $LiClO_4$ in the range 915–955 cm^{-1} (after

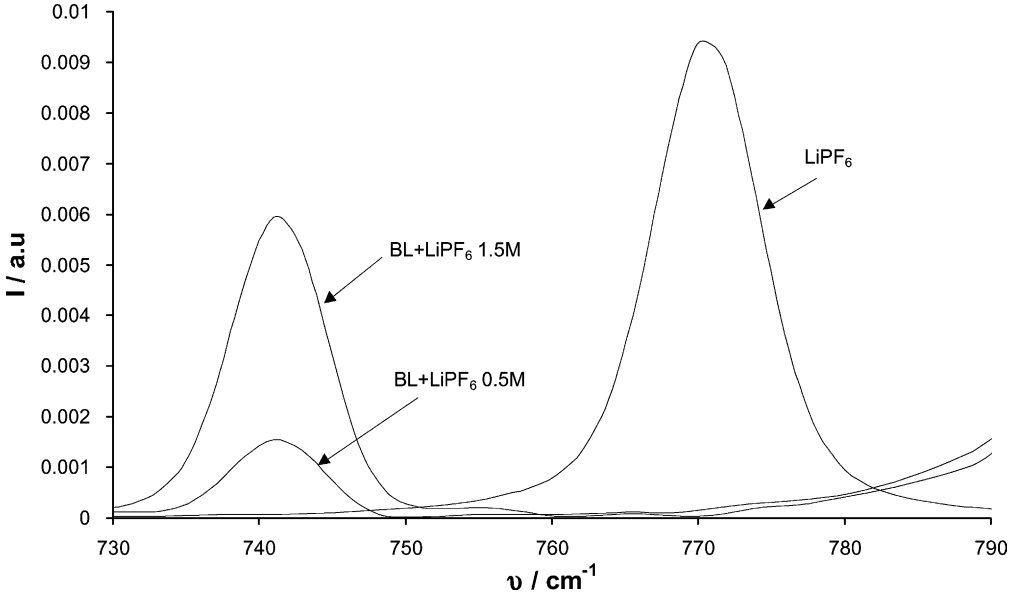

Fig. 9. Raman spectra of solid $LiPF_6$ (as powder), $LiPF_6$ (0.5 M) and $LiPF_6$ (1.5 M) in BL.

subtracting and normalising the spectra as indicated in the experimental part). An unperturbed perchlorate anion has a tetrahedral structure and belongs to T_d symmetry group. The nine vibrational degrees of freedom are divided into four modes of vibration [29]: $\upsilon_1(A_1) = 931\ cm^{-1}$, $\upsilon_2(A_2) = 458\ cm^{-1}$, $\upsilon_3(F_2) = 1100\ cm^{-1}$, $\upsilon_4(F_2) = 624\ cm^{-1}$. All the four modes are Raman-active and F_2 is IR-active. In $LiClO_4$ acetone solutions, the following species have been observed [30]: free ions ClO_4^- ($933\ cm^{-1}$), contact ions pairs $[Li^+ \ldots ClO_4^-]$ ($955\ cm^{-1}$) and solvent separated ions pairs ($948\ cm^{-1}$). The Raman spectrum of $LiClO_4$ in BL, reported in Fig. 10, shows the presence of only two emission bands which have been attributed to free ions and ion-pairs. The exact nature of the ion-pairs is not known. Using the emission at the preceding wavelength, the dissociation coefficient α of $LiClO_4$ in BL has been evaluated as a function of the salt concentration. The α values, reported in Table 7, exhibit little variations when the salt concentration of the is raised from 0.1 to 1.5 M as the precision of the measurements is of the order of ± 0.05. As a consequence, the cube root law, Eq. (3), remains applicable and only the slope of the $\Lambda = f(C^{1/3})$ relation will be affected by the presence of ion-pairs.

The formation of loose ion-pairs (solvent separated or solvent–solvent separated ion-pairs) is highly probable even

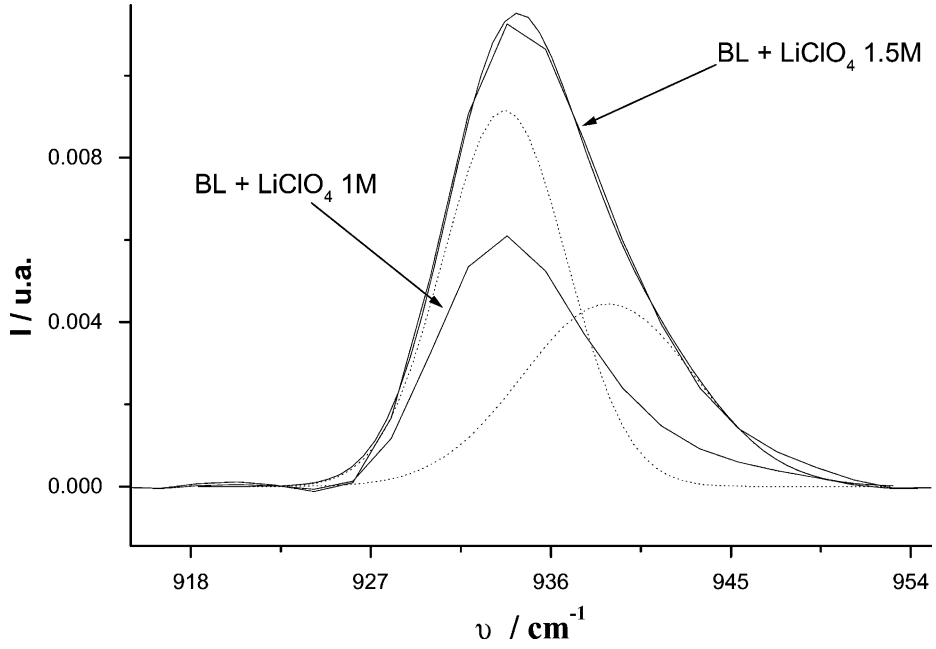

Fig. 10. Raman spectra of BL without salt and with added $LiClO_4$ (1 M and 1.5 M) in the 915–955 cm^{-1} range.

Table 7
Dissociation degrees of $LiClO_4$ in BL at 25 °C determined by Raman spectroscopy

C/M	α ($LiClO_4$)
0.10	0.54
0.20	0.46
0.50	0.67
0.75	0.64
1.00	0.65
1.50	0.55

in high permittivity organic electrolytes, but their detection by Raman spectrometry cannot be always achieved, as the emission bands of anions are only sligthly affected by ion pairing in this case. In any case, their presence is not in conflict with the quasi-lattice structure of the electrolyte as these species are only temporarily formed and can be considered as defects in the quasi-lattice structure of the electrolyte solution.

4. Conclusion

The aim of this work is to highlight the transport properties, viscosity and conductivity, of concentrated organic electrolytes. The duality between Λ and η, found in the Walden product W for example, find an easy interpretation in terms of the transition state theory when the activation energies for conductivity and viscosity have similar values [31]. The quasi-lattice model, widely used in fused salt studies, can be successfully extended to concentrated organic electrolytes involving strongly dipolar aprotic solvents.

The coulombic interactions between neighbouring ions on which this model is based, are able to explain the variation of the molar conductivity Λ and its activation energy $E_{a,\Lambda}$ when the concentration of the salt is varied. The same forces are at the origin of the increase in viscosity η of the electrolyte which is well described by the JD semi-empirical law. The bell shape, usually observed for the $K = f(C)$ plot in dipolar aprotic solvents is well in accordance with the cube root law for Λ. The predictive character of the model is potentially interesting as the only adjustable parameter M, the lattice parameter has been found to vary only moderately from the fcc value. Combination of the Walden product and of the JD equation shows that the concentration in salt at the maximum of conductivity C_{max} is strongly related to the D-coefficient and, hence to ion–ion interactions.

The association of ions in pairs, as observed by Raman spectroscopy for $LiClO_4$ in BL, does not invalid the use of the cube root law as it has been found that the dissociation coefficient remains constant in the concentration range 0.5–1 M. Others associated species than contact ion-pairs may be considered as defects in the quasi-lattice structure of the electrolyte solution.

Acknowledgements

A. Chagnes will express thanks to Region Centre council for financial support and sincerely thanks to Prof. Pierre Dubois and Laurence Douziech-Eyrolles (University of Tours) for discussions about Raman spectroscopy.

References

[1] G. Jones, M. Dole, J. Am. Chem. Soc. 51 (1929) 2950;
M. Kaminsky, Z. Physik. Chem. Neue Folge 5 (1955) 164;
M. Kaminsky, Z. Physik. Chem. Neue Folge 12 (1957) 206.
[2] H. Falkenhagen, Z. Physik. 32 (1931) 3655;
H. Falkenhagen, E.L. Vernon, Z. Physik. 33 (1932) 140.
[3] N.C. Dey, G. Kumar, B.K. Saika, I. Haque, J. Sol. Chem. 14 (1985) 49;
D.J.P. Out, J.M. Los, J. Sol. Chem. 9 (1980) 19.
[4] M.M. Lencka, A. Anderko, S.J. Sanders, R.D. Young, Int. J. Thermophys. 19 (1998) 367.
[5] L. Onsager, Phys. Z. 27 (1926) 388.
[6] J.-C. Justice, in: B.E. Conway, J.O'M. Bockris, E. Yeager, (Eds.), Comprehensive Treatise of Electrochemistry, Vol. 5, Plenum Press, New York, 1983, Chapter 3.
[7] A. Chagnes, B. Carre, P. Willmann, D. Lemordant, Electrochim. Acta 46 (2001) 1783.
[8] D. Brouillette, G. Perron, J. Desnoyers, Electrochim. Acta 44 (1999) 4721.
[9] Y. Aihara, K. Sugimoto, W.S. Ptice, K. Hayamizu, J. Chem. Phys. 113 (2000) 1981–1991.
[10] C. Ghosh, J. Chem. Soc. 113 (1918) 449.
[11] I. Ruff, G. Palinkas, K. Combos, J. Chem. Soc., Faraday Trans. 2 77 (1981) 1189.
[12] R.A. Robinson, R.H. Stokes, "Electrolyte solutions", 2nd Edition, Butterworth, London, 1959, p. 226.
[13] M. Salomon, E.J. Plitcha, Electrochim. Acta 138 (1991) 2586.
[14] S.A. Agnihotry, Nidhi, P. Pradeep, S.S. Sekhon, Solid State Ionics 136/137 (2000) 573–576.
[15] D. Feakins, D.J. Freemantle, K.G. Lawrence, J. Chem. Soc., Faraday Trans. 1 70 (1974) 795.
[16] J.E. Desnoyers, G. Perron, J. Sol. Chem. 1 (1972) 199.
[17] A. Einstein, Ann. Phys. 19 (1906) 289;
A. Einstein, Ann. Phys. 34 (1911) 591.
[18] M. Ue, J. Electrochem. Soc. 145 (1998) 3336.
[19] J.F. Kincaid, H. Eyring, A.E. Stearn, Chem. Rev. 28 (1941) 301.
[20] L.W. Bahe, J. Phys. Chem. 76 (1972) 1608.
[21] G.W. Murphy, J. Chem. Soc., Faraday Trans. 2 79 (1983) 1607.
[22] F.W. Smith, Cell Theory of electrolyte solutions, Ph.D. Dissertation, University of Ohklahoma, 1963 University microfilm International, Ann Arbor, MI 48106, USA, 6303705, p. 13.
[23] A. Chagnes, unpublished data.
[24] K. Hayamizu, Solid State Ionics 107 (1998) 1.
[25] N. Bjerrum, Kon. Danske. Videnk. Selskab 9 (1926) 7.
[26] L. Doucey, Coll. Electrochim. Acta 44 (1999) 2371.
[27] D. Battisti, G.A. Nazri, B. Klassen, R. Acorsa, J. Phys. Chem. 92 (1993) 5826.
[28] M. Caillon-Caravanier, J. Electrochem. Soc., in press. Manuscript number: JES 01-11-026.
[29] Z. Wang, J. Electrochem. Soc. 145 (1998) 3346.
[30] D.W. James, Aust. J. Chem. 35 (1982) 1775.
[31] I. Geoffroy, P. Willmann, K. Mesfar, B. Carré, D. Lemordant, Electrochim. Acta 45 (2000) 2019.